

## Systematics of Feshbach resonances in the molecular halogens\*

David Spence

Argonne National Laboratory, Argonne, Illinois 60439

(Received 28 May 1974)

Using an electron transmission spectrometer the energetically lowest-lying Feshbach resonances in the molecular halogens  $F_2$ ,  $Cl_2$ ,  $Br_2$ , and  $I_2$  are located. These resonances are associated with Rydberg states and have symmetry  $(X^2\Pi_g)(ns\sigma)^2 [^2\Pi_{1/2,3/2}]$ , where  $n = 3, 4, 5$ , and  $6$  for  $F_2$ ,  $Cl_2$ ,  $Br_2$ , and  $I_2$ , respectively. The binding energy of the lowest pair of  $ns\sigma$  electrons to the ground-state positive ion core decreases monotonically as the size of the molecules increases from  $4.45 \pm 0.05$  eV in fluorine to  $3.57 \pm 0.05$  eV in iodine. A simple qualitative theoretical argument, based on an atomic model, satisfactorily describes the decrease in the binding energy.

### I. INTRODUCTION

It was suggested by Weiss and Krauss,<sup>1</sup> and convincingly demonstrated by Sanche and Schulz,<sup>2</sup> that excited Rydberg states of molecules (but not valence states) can support core-excited Feshbach resonances. The temporary negative-ion complex formed consists of two Rydberg electrons moving in the (mainly Coulomb) field of the ion core. The physical reason for such a configuration is that negative ions with two excited electrons of the same principal quantum number are more stable than other configurations because of minimized mutual screening; two electrons with different principal quantum numbers will not realize a bound complex because of the extensive screening of one electron by the other. Rydberg electrons are essentially nonbonding, and thus the nuclear motion in the ion core remains unperturbed by the addition of two extra electrons. Specifically, the vibrational spacings and Franck-Condon factors (and hence the observed vibrational intensities) are similar for vibrational progressions associated with formation of both the negative-ion and the positive-ion grandparent. It was this fact that enabled Sanche and Schulz<sup>2</sup> to establish that Feshbach resonances are indeed usually associated with Rydberg states and not with valence states.

Since the pioneering work of Sanche and Schulz,<sup>2</sup> vibrational progressions of resonances in many other molecules have been identified and interpreted using this model.<sup>3-5</sup> We use the same arguments in the present paper to determine the grandparentage of the observed resonances. It has recently been pointed out by Schulz<sup>5</sup> that in all the diatomic molecules in which Feshbach resonances have been observed to date, the binding of the lowest pair of  $ns\sigma$  electrons to the positive-ion grandparent state is always  $4.0 \pm 0.1$  eV. In addition, the binding of the lowest pair of  $ns$  electrons

to the positive-ion core in atoms is also usually  $4.1 \pm 0.1$  eV,<sup>5</sup> though for atoms exceptions to this rule have been noted.<sup>5,6</sup>

Actually the  $4.1 \pm 0.1$  eV binding-energy "rule" for the lowest pair of  $ns\sigma$  electrons is a consequence of the fact that to date studies of Feshbach resonances in diatomic molecules have been restricted to molecules composed of atoms in the first two rows of the periodic table. In the present paper we study the binding energies of the lowest pair of  $ns\sigma$  Rydberg electrons to positive-ion cores for  $F_2$ ,  $Cl_2$ ,  $Br_2$ , and  $I_2$ . Thus, we are able to elucidate the systematics of Feshbach resonances down a column of the periodic table. The binding energy of the lowest pair of  $ns\sigma$  electrons to the grandparent state varies from 4.5 to 3.5 eV as the principal quantum number of the lowest pair of  $ns\sigma$  electrons varies from 3 to 6. We present a simple physical model to explain this decrease in the binding energy as the size of the molecule increases. In addition, studies of vibrational progressions of Feshbach resonances in molecules give information concerning the nature of those Rydberg states whose optical excitation is forbidden by selection rules.

### II. APPARATUS

For the present experiments, an electron transmission spectrometer, similar to that described by Sanche and Schulz,<sup>7</sup> has been used. The principles of the apparatus, shown in Fig. 1, have been discussed previously in great detail,<sup>7</sup> so only a brief description will be given here.

Electrons are emitted from a thorium-coated iridium filament, and an electron beam with an energy spread of about 60 meV is selected by a trochoidal monochromator (TM).<sup>8</sup> The electron beam, confined by a magnetic field  $B$ , is accelerated into the collision chamber  $C$ , where it intersects a molecular beam. Electrons which have

their velocity vector reoriented in a collision with a gas molecule in the beam are retarded by a potential  $V_r$ , applied to the retarding electrode  $R$ , and the unscattered electrons are collected by the collector (EC). The microwave cavity in the gas line in Fig. 1 can be used for producing free radicals, though this facility is not used in the present experiments. Using the technique described by Sanche and Schulz,<sup>7</sup> the electron energy in the collision chamber is modulated, and the modulated component of the transmitted current is measured with a phase-sensitive detector. This technique has the advantage of greatly suppressing the slowly varying background due to "direct" scattering and enhancing structures due to scattering of electrons via a resonance process.

Our energy scale is determined by reference to the  $1s2s^2(^2S)$  resonance in helium, which is known to occur at  $19.355 \pm 0.008$  eV.<sup>9</sup> The purity of all the gases used was specified by the manufacturers as better than 99.5%. No attempts were made at further purification.

### III. RESULTS

#### A. Fluorine

An  $x$ - $y$  plot of the derivative of the transmitted current in molecular fluorine with respect to the incident electron energy between 10.5 and 12.5 eV is shown in Fig. 2. This plot shows two progressions of resonances starting at 11.25 and 11.90 eV. Following the criteria of Sanche and Schulz<sup>3</sup> for selection of resonance centers in a vibrational progression, we have marked the resonance positions by the vertical straight lines. The vibrational quantum numbers of these resonances are indicated by the numbers above the straight lines, and the separation between adjacent levels appears between them. For the first series of resonances, band  $a$ , the vibrational structures are of equal spacing (130 meV), in con-

trast to the second series, band  $b$ , where there is a marked anharmonicity.

Though Fig. 2 represents the derivative of the transmitted current, relative vibrational intensities of the resonance peaks may still be obtained from the height of the observed structures, provided the lifetime against autoionization of the state is independent of the vibrational quantum number. To the extent that the experimentally observed width of the structures is independent of the vibrational quantum number, this requirement is fulfilled. The average spacing of 0.130 eV between adjacent vibrational resonances of band  $a$  in Fig. 2 is almost exactly the same as the vibrational spacings of the  $X^2\Pi F_2^+$  ion which has been spectroscopically determined to be 0.132 eV.<sup>10,11</sup>

The vibrational intensities for the  $F_2^-$  states of band  $a$  obtained in the present experiment are compared in Table I with the vibrational intensities for the  $X^2\Pi F_2^+$  state, derived from the data of Potts and Price<sup>10</sup> and of Cornford *et al.*<sup>11</sup> The agreement between the vibrational intensities for the negative- and positive-ion systems is considered to be sufficiently good for assigning the  $X^2\Pi F_2^+$  state as the grandparent state of band  $a$  in Fig. 2. The measured spin-orbit splitting  $^2\Pi_{3/2} - ^2\Pi_{1/2}$  of the positive-ion core is 0.030 eV.<sup>10,11</sup> This splitting is too small to be detected using the resolution that the present apparatus could provide in the presence of such a reactive gas as fluorine. However, we have marked the expected locations of the  $^2\Pi_{1/2}$  component also in Fig. 2.

For band  $b$ , consideration of any excited positive-ion core as the grandparent state would lead to binding energies for the pair of electrons which were unrealistically high. Consequently, we suggest that the grandparent of band  $b$  is also the  $X^2\Pi F_2^+$  state, but with different configurations of the two additional electrons from band  $a$ . This will be discussed in greater detail in Sec. IV of this paper.

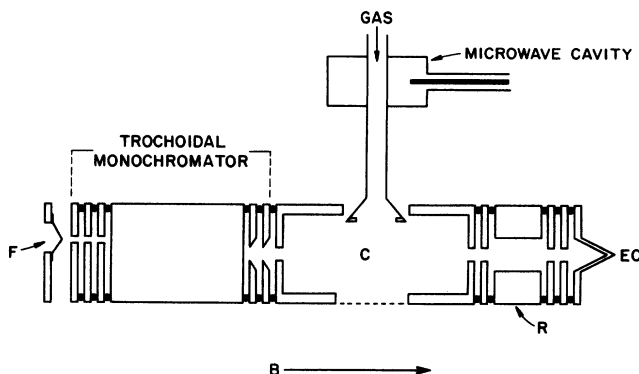


FIG. 1. Schematic diagram of the apparatus.

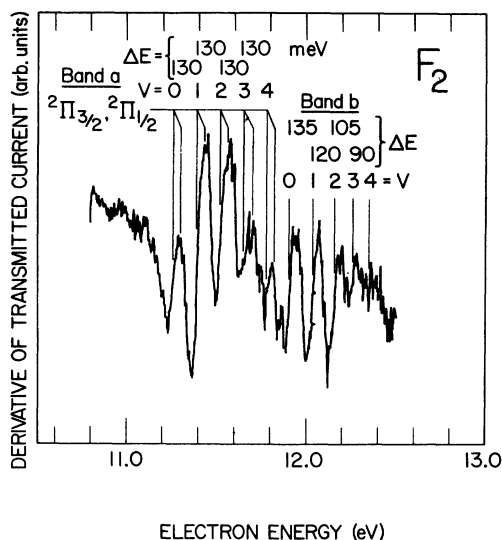


FIG. 2. Derivative of the transmitted electron current vs electron energy in molecular fluorine. Band *a* derives from addition of two  $n s \sigma$  electrons to the  $X^2\Pi_g$  positive-ion core. Band *b* derives from the addition of one  $n s \sigma$ , plus one  $n p \sigma$  or  $n p \pi$  electron to the same positive-ion core.

### B. Chlorine

The derivative of the transmitted current in molecular chlorine between 7.0 and 9.0 eV is shown in Fig. 3. This plot shows a progression of six resonances starting at 7.46 eV. The resonance centers of the vibrational progression are again marked by the vertical straight lines, and the vibrational quantum numbers of these resonances are indicated by the numbers above the straight lines. The separation between adjacent levels appears between them. There is no measurable anharmonicity in this vibrational progression.

The average spacing between adjacent resonances, 80 meV, is the same as the vibrational spacings of the  $X^2\Pi$   $Cl_2^+$  ion, which has been spectroscopically<sup>10,11</sup> determined to be 0.080 eV. The anharmonicity in the  $X^2\Pi$   $Cl_2^+$  state is a mere 2.9  $cm^{-1}$ , which precludes measurement in an electron scattering experiment.

The vibrational intensities for the  $Cl_2^-$  states obtained in the present experiments are compared in Table I with those for the  $X^2\Pi$   $Cl_2^+$  state, derived from the data of Potts and Price<sup>10</sup> and of Cornford *et al.*<sup>11</sup> Despite the difficulties in extracting approximate vibrational intensities from

TABLE I. Comparison of vibrational intensities observed for progressions of Feshbach resonances in the present experiments with the appropriate vibrational intensities observed for the molecular halogen ( $X^2\Pi$ ) positive-ion states.

Vibrational quantum number	Negative-ion system Present experiment	Vibrational intensities	
		Positive-ion system	
		Potts and Price <sup>a</sup>	Cornford <i>et al.</i> <sup>b</sup>
	$F_2(^4\Sigma_g^+, v=0) \rightarrow F_2^-(v)$	$F_2(^4\Sigma_g^+, v=0) \rightarrow F_2^+(X^2\Pi, v)$	
0	0.44	0.59	0.53
1	1.00	1.00	1.00
2	0.72	0.66	0.66
3	0.22	0.19	0.25
4	0.13	0.11	0.09
	$Cl_2(^4\Sigma_g^+, v=0) \rightarrow Cl_2^-(v)$	$Cl_2(^4\Sigma_g^+, v=0) \rightarrow Cl_2^+(X^2\Pi, v)$	
0	0.42	0.46	0.39
1	0.89	0.88	0.91
2	1.00	1.00	1.00
3	0.83	0.74	0.63
4	0.50	0.36	0.23
5	0.19	0.16	0.11
	$Br_2(^4\Sigma_g^+, v=0) \rightarrow Br_2^-(v)$	$Br_2(^4\Sigma_g^+, v=0) \rightarrow Br_2^+(X^2\Pi, v)$	
0	0.70	0.53	0.57
1	1.00	1.00	1.00
2	0.67	0.84	0.77
3	0.51	0.44	0.40
4	0.25	0.31	0.17

<sup>a</sup>Reference 10.

<sup>b</sup>Reference 11.

the present data because of the rapidly rising background in Fig. 3, the agreement between the negative and positive ions is considered to be good. Though the spin-orbit splitting of the positive-ion core in chlorine (0.080 eV) is larger than in fluorine, spectroscopic measurement shows that this splitting is exactly equal to the vibrational spacing,<sup>10,11</sup> thus precluding observation in the present experiment.

### C. Bromine

The derivative of the transmitted electron current through molecular bromine with respect to the incident electron energy between 6.5 and 7.5 eV is shown in Fig. 4. In this plot, two vibrational progressions occur, beginning at 6.720 and 7.065 eV, respectively. The spacing between the vibrational levels of both series is 0.045 eV, to be compared with that of 0.045 eV for the vibrational spacings of the  $X^2\Pi\text{Br}_2^+$  ion state obtained by photoelectron spectroscopy.<sup>10,11</sup>

The comparison of vibrational intensities for the negative- and positive-ion system in Table I for  $\text{Br}_2$  may be of questionable value in view of the rapidly increasing backgrounds of Fig. 4. However, the agreement between the vibrational spacings in the negative- and positive-ion system, together with the agreement between the  $^2\Pi_{3/2} \rightarrow ^2\Pi_{1/2}\text{Br}_2^+$  spin-orbit splitting (0.350 eV)<sup>10,11</sup> and the measured separation of the two bands of Fig.

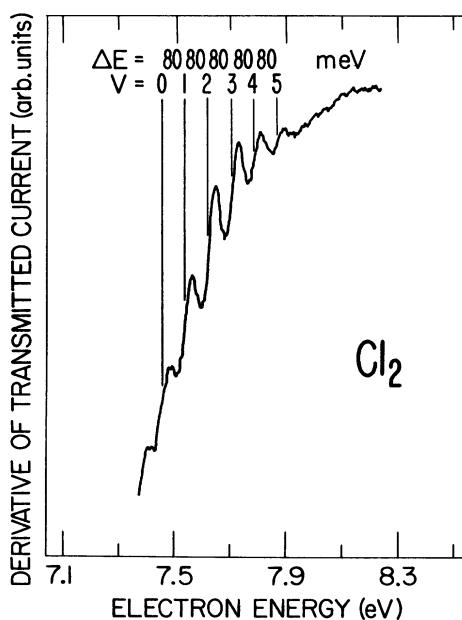


FIG. 3. Derivative of the transmitted electron current vs electron energy in molecular chlorine. This band of resonances derives from the addition of two  $n\sigma$  electrons to the  $X^2\Pi_g$  positive-ion core.

4 (0.345 eV) provide convincing evidence that the  $X^2\Pi\text{Br}_2^+$  state is indeed the grandparent of the observed resonances in bromine.

### D. Iodine

The derivative of the transmitted electron current through molecular iodine with respect to the incident electron energy between 4.5 and 7.5 eV is shown in Fig. 5. In this plot are shown two large resonances located at 5.78 and 6.38 eV, together with two smaller resonances located at 6.850 and 7.150 eV. Vibrational structures in the  $I_2^-$  states are too closely spaced to be resolved in the present experiment. Cornford *et al.*<sup>11</sup> have partially resolved three vibrational levels of the  $^2\Pi_{1/2}$  component of the  $^2\Pi I_2^+$  state by photoelectron spectroscopy and find the vibrational spacing to be 0.030 eV.

However, we can compare the ratio of the magnitude of the two large resonances of Fig. 5, 0.83, with the ratio of the magnitude of the  $^2\Pi_{3/2}$  and  $^2\Pi_{1/2}$  bands of the  $X^2\Pi I_2^+$  ion, 0.78, obtained by photoelectron spectroscopy.<sup>12</sup> This agreement, together with the similarity between the  $^2\Pi_{3/2} \rightarrow ^2\Pi_{1/2} I_2^+$  splitting (0.650 eV), and resonance separation (0.600 eV), provide good evidence for assigning the  $X^2\Pi I_2^+$  state as the grandparent of the two resonances located at 5.78 and 6.38 eV. By

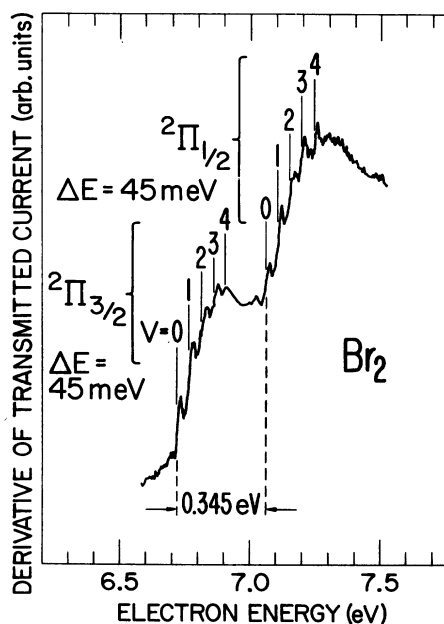


FIG. 4. Derivative of the transmitted electron current vs electron energy in molecular bromine. The two bands of resonances derive from the addition of a pair of  $n\sigma$  electrons to the  $^2\Pi_{3/2}$  and  $^2\Pi_{1/2}$  components of the  $X^2\Pi_g$  positive-ion core. The separation of the two bands, 0.345 eV, is indicated by the horizontal arrows.

similar arguments to those advanced for band *b* of fluorine, we suggest that the two resonances located at 6.85 and 7.15 eV also have  $X^2\Pi I_2^+$  as their grandparent. Though the separation of these two resonances is less than the two lower resonances, this may be expected if the two electrons bound to the ion core are not equivalent in this case. Possible configurations of these states will be discussed in Sec. IV.

#### IV. DISCUSSION

In order to determine the electron configurations of the observed resonances, it is first necessary to determine the configurations of the parent Rydberg states with which they are associated. Unfortunately, the lowest Rydberg states in the halogens cannot be studied by usual optical methods. Absorption of radiation from the ground state, or emission to the ground state, is forbidden by parity considerations.<sup>12</sup> In 1947, Venkateswarlu<sup>13,14</sup> studied emission from some optically forbidden states of  $Br_2$  and  $I_2$  to several dissociating states. In more recent papers,<sup>15,16</sup> Venkateswarlu has reinterpreted part of his data and tentatively assigned some of these forbidden states

as low-lying Rydberg states. The energies of these forbidden states were determined by averaging the energies of several emission lines which differed by as much as  $3000\text{ cm}^{-1}$ . Such crude approximations render the optical data useless for our present requirements. However, other means are available for determining the probable parent Rydberg states of the observed resonances.

In the following discussion we will regard the formation of the negative-ion system as an electron attaching to an already existing Rydberg state, although a more realistic picture would be to consider excitation and attachment simultaneously. This approach is satisfactory for explaining systematics of Feshbach resonances in relation to the ionization potentials,<sup>11,12</sup> and avoids the difficult problem of handling two excited electrons simultaneously, together with their associated mutual screening of the ion core.

The binding energies  $E_B$  of a pair of Rydberg electrons moving in the field of a positive-ion core can be approximated by

$$E_B = R/(n - \mu)^2 + I, \quad (1)$$

where  $n$  is the principal quantum number of the Rydberg electron,  $\mu$  is its quantum defect,  $I$  is the electron affinity of the neutral Rydberg state, and  $R$  is the Rydberg energy. In the molecular halogens the lowest excited electrons may be in  $ns\sigma$ ,  $np\sigma$ , or  $np\pi$  orbitals, where  $n$  takes the value 3, 4, 5, and 6, for  $F_2$ ,  $Cl_2$ ,  $Br_2$ , and  $I_2$ , respectively. A knowledge of the electron affinities, and (more critically) the quantum defects of these states, would immediately enable us to identify which Rydberg states the observed resonances are associated with. The quantum defect ( $\mu$ ) of a Rydberg state is equivalent to  $\delta$ , the asymptotic phase shift ( $\pi\mu = \delta$ ) of the excited electron relative to an equivalent electron moving in a Coulomb field.<sup>17</sup>

Asymptotic phase shifts for  $s$ ,  $p$ , and  $d$  electrons moving in the field of atomic ions have recently been calculated by Dehmer and Saxon.<sup>18</sup> These calculations, based on the Hartree-Slater model, were performed for all atoms in the first two rows of the periodic table and for a range of principal quantum numbers 1 to 10. Similar calculations have also been made for Br and I atoms.<sup>19</sup>

The atomic quantum defects serve as a guide for selection of molecular quantum defects. Comparison of known quantum defects for homonuclear diatomic molecules<sup>20,21</sup> with calculated atomic quantum defects<sup>18</sup> show that the two usually differ by only (5–10)%. This is especially true of second-row elements. This is not so surprising as it seems, since that part of the quantum defect

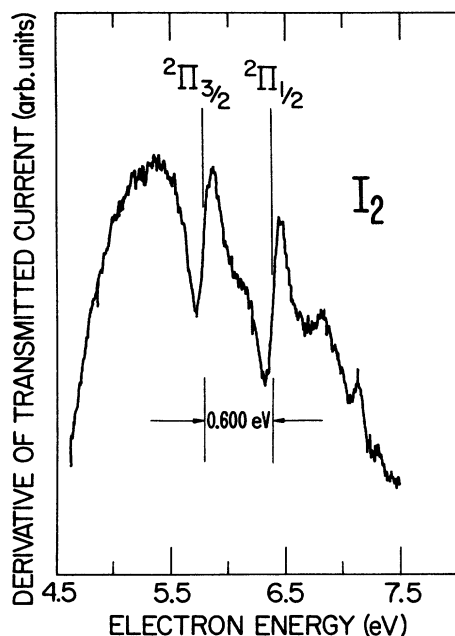


FIG. 5. Derivative of the transmitted electron current vs electron energy in molecular iodine. The two large resonances, split by 0.600 eV, derive from the addition of a pair of  $ns\sigma$  electrons to the  $2\Pi_{3/2}$  and  $2\Pi_{1/2}$  components of the  $X^2\Pi_g$  positive-ion core. Observation of vibrational structures in molecular iodine is precluded by the small separation of vibrational levels in the positive-ion core.

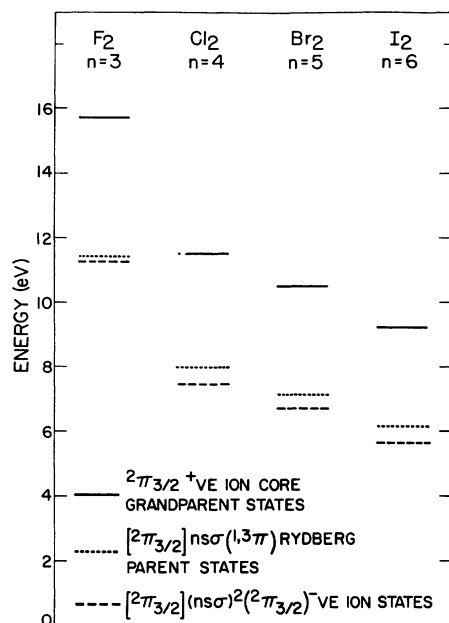


FIG. 6. Energy-level diagram showing the locations of experimentally observed ionization potentials and lowest-energy Feshbach resonances in  $F_2$ ,  $Cl_2$ ,  $Br_2$ , and  $I_2$ . The locations of the lowest Rydberg states, estimated from calculated atomic quantum defects, are shown by the dashed lines. With the exception of  $F_2$ , which is anomalous in almost every physical property, the electron affinity of the lowest Rydberg state in all molecules is very close to 0.5 eV.

which derives from closed shells is not strongly affected by the molecular field. The molecular field alters the quantum defect only by virtue of its effect on the redistribution of the valence shell. We have used the calculated atomic quantum defects<sup>18</sup> to estimate the binding energies of the lowest Rydberg electrons (most tightly bound) in the molecular halogens. According to Eq. (1), the results of this estimate are shown in Fig. 6. In this figure the solid lines are the ionization energies of the molecular halogens obtained from photoelectron spectroscopy by Potts and Price.<sup>10</sup>

The dashed lines are the location of the lowest resonance of each band obtained in the present experiments.<sup>22</sup> The dotted lines indicate the location of possible parent Rydberg states obtained from the above calculations. It is clear from Fig. 6 that the only reasonable parentage of the lowest observed resonances is derived from addition of an electron of  $ns\sigma$  symmetry to the  $X^2\Pi_g$  ion cores, giving a Rydberg state with configuration  $[X^2\Pi_g]ns\sigma^1,^3\Pi_g$ . In all cases except fluorine, the electron affinity of the Rydberg states is seen to be of the order of 0.5 eV. From studies of Feshbach resonances in many atoms and molecules, it is found that, for an additional electron with zero angular momentum, the binding energy is usually  $0.5 \pm 0.1$  eV. The addition of a second electron of  $ns\sigma$  symmetry to the  $1,^3\Pi_g$  Rydberg parent states will cause the two Rydberg electrons to form a pair (spins antiparallel) giving  $[X^2\Pi_g](ns\sigma)^2\Pi_g$  negative-ion states. In Fig. 6 only the lowest,  $^2\Pi_{3/2}$ , of the two spin-orbit components have been indicated.

The assumption that the reinterpretation of emission spectra of  $I_2$  and  $Br_2$  by Venkateswarlu<sup>13-16</sup> is correct would lead to an electron affinity of the lowest Rydberg state in  $Br_2$  ( $[X^2\Pi_g]5s\sigma^1,^3\Pi$ ) of 0.17 eV (unreasonably low for an s electron) and in  $I_2$  ( $[X^2\Pi_g]6s\sigma^1,^3\Pi$ ) of 0.74 (rather high). This leads us to the conclusion either that wrong configurations have been assigned<sup>15,16</sup> to some emission lines of  $I_2$  and  $Br_2$ , or (more probably) that the experimental technique used in those studies<sup>13,14</sup> leads to ill-defined energetics. From arguments similar to those above, we propose that band *b* of  $F_2$ , and the 6.85-eV and 7.15-eV resonances in  $I_2$  occur by the addition of one  $ns\sigma$  electron plus one  $np\sigma$  or  $np\pi$  electron to the  $[X^2\Pi_g]$  positive-ion core, giving configuration  $[X^2\Pi_g]np\sigma(\pi),ns\sigma$ . At present we are not able to say whether the Rydberg electron has  $np\sigma$  or  $np\pi$  symmetry, as the ordering of those levels does not always occur as predicted by simple theory.<sup>23,24</sup> Molecular chlorine and bromine also should un-

TABLE II. Tabulation of ionization potentials and lowest observed Feshbach resonances in the molecular halogens, together with the binding energies of the lowest pair of  $ns\sigma$  electrons to the positive-ion core in these molecules.

Molecule	Ionization potential (eV)		Resonance energy (eV) Present experiment	Resonance principal quantum number	$(ns\sigma)^2$ binding energy (eV)
	Potts and Price <sup>a</sup>	Cornford <i>et al.</i> <sup>b</sup>			
$F_2$	15.70	15.7	11.25	3	4.45
$Cl_2$	11.51	11.49	7.46	4	4.05
$Br_2$	10.51	10.51	6.72	5	3.79
$I_2$	9.35 (vertical)	9.34	5.78 (vertical)	6	3.57
	9.33 (adiabatic)		5.65 (adiabatic)		

<sup>a</sup>Reference 10.

<sup>b</sup>Reference 11.

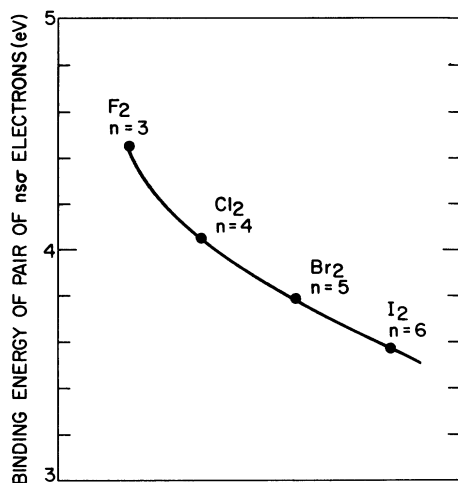


FIG. 7. Binding energies of the lowest pair of  $ns$  electrons to ground-state positive-ion cores for the molecular halogens. The binding energy of the  $ns$  pair decreases monotonically by almost 1 eV as the molecular size increases from fluorine to iodine.

doubtedly have resonances with analogous configurations, but preclude a search because of extreme difficulty in maintaining sufficient resolution in the presence of these gases.

It is seen from Fig. 6 that the binding energies of the pair of  $ns$  electrons (where  $n=3, 4, 5$ , and 6 for  $F_2$ ,  $Cl_2$ ,  $Br_2$ , and  $I_2$ , respectively) to the  $X^2\Pi_g$  positive-ion core is not independent of the molecular species, as has often been noted in the past for diatomic molecules. The variation in binding energy of the electron pair as one moves down a column of the periodic table is tabulated in Table II and is illustrated more clearly in Fig. 7. Figure 7 shows the variation in the binding energy between  $F_2$  and  $I_2$  to be almost 1 eV, much greater than the previously observed variation of  $\pm 0.1$  eV. As we move from a molecule in one row of the periodic table to a molecule in the adjacent row but the same column, the principal quantum number  $n$  of the lowest-lying Rydberg electron [Eq. (1)] will increase by unity. However, there also exists an extra closed shell and an additional loop (additional phase shift of  $\pi$ ) in the Rydberg electron's wave function. This causes  $\mu$ , the quantum defect, to increase by unity, making the first term on the right-hand side of Eq. (1) independent of the species of halogen. Furthermore, the data of Fig. 6 imply that the rule  $0.5 \pm 0.1$  eV for the electron affinities of Rydberg states for an  $s$  electron is essentially independent of the species of halogen. The problem is not why the binding energy of the electron pair is always 4.1 eV, but rather why it is *not* always 4.1 eV.

The physical reasons for the variation are best explained with reference to Fig. 8. Here we have

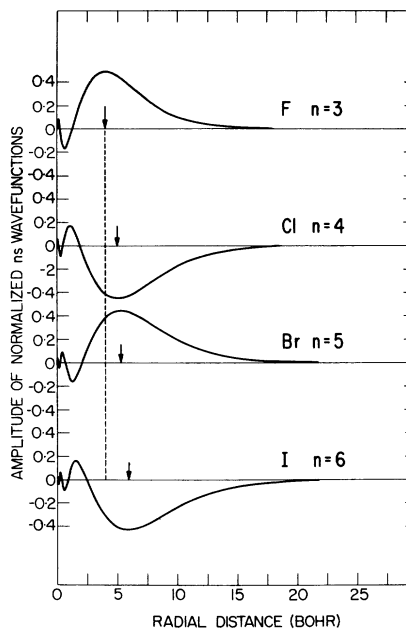


FIG. 8. Hartree-Slater radial wave functions for the lowest  $ns$  Rydberg electrons in F, Cl, Br, and I. The radial coordinates of the extrema of the largest loops are indicated by the arrows, and show the increase in size of the electron orbit from F through Cl and Br to I.

plotted Hartree-Slater radial wave functions for the lowest  $ns$  Rydberg electrons moving in the field of the positive-ion core for the atoms F, Cl, Br, and I. Figure 8 shows that as we move down the halogen column, at each step filling an extra shell, the innermost shells shrink. However, the largest loop of the wave function, where the Rydberg electron spends most time, is not exactly at the same radial distance for all atoms, but actually increases slightly from F through Cl and Br to I. The outermost loop increases in distance from the core as the shells progressively fill because the wave functions are more and more excluded from the core by orthogonality to the innermost  $s$ -electron wave functions.

Thus, as one descends the halogen column, the principal quantum number of the first excited Rydberg state increases by unity, but, owing to the monotonic increase of atomic "size" due to increasing core "size," the quantum defect steps by an amount slightly less than unity. Hence, in this sequence, the binding energy of a pair of  $ns$  electrons moving in the field of a positive ion will decrease. This is consistent with experiment.

Though this model discusses atoms, the same arguments should apply to molecules. For now, we have no sufficiently accurate molecular wave functions to illustrate this effect.

## ACKNOWLEDGMENTS

The author is indebted to Dr. J. L. Dehmer for help in theoretical interpretation and especially for communicating unpublished results on atomic wave functions. Helpful discussions with Dr. W. A. Chupka and Dr. M. Inokuti are also greatly appreciated.

---

\*Work performed under the auspices of the U. S. Atomic Energy Commission.

<sup>1</sup>A. W. Weiss and M. Krauss, *J. Chem. Phys.* **52**, 4363 (1970).

<sup>2</sup>L. Sanche and G. J. Schulz, *Phys. Rev. Lett.* **27**, 1333 (1971).

<sup>3</sup>L. Sanche and G. J. Schulz, *Phys. Rev. A* **6**, 69 (1972).

<sup>4</sup>L. Sanche and G. J. Schulz, *J. Chem. Phys.* **58**, 479 (1973).

<sup>5</sup>G. J. Schulz, *Rev. Mod. Phys.* **45**, 378 (1973).

<sup>6</sup>D. Spence and W. A. Chupka, *Phys. Rev. A* **10**, 71 (1974).

<sup>7</sup>L. Sanche and G. J. Schulz, *Phys. Rev. Lett.* **26**, 943 (1971).

<sup>8</sup>A. Stamatovic and G. J. Schulz, *Rev. Sci. Instrum.* **41**, 423 (1970).

<sup>9</sup>S. Cvejanovic, J. Comer, and F. H. Read, in *Proceedings of the Eighth International Conference on the Physics of Electronic and Atomic Collisions, Beograd, 1973* (Institute of Physics, Beograd, 1973), p. 441.

<sup>10</sup>A. W. Potts and W. C. Price, *Trans. Faraday Soc.* **67**, 1242 (1971).

<sup>11</sup>A. B. Cornford, D. C. Frost, C. A. McDowell, J. L. Rayle, and I. A. Stenhouse, *J. Chem. Phys.* **54**, 2651 (1971).

<sup>12</sup>G. Herzberg, *Spectra of Diatomic Molecules* (Van Nostrand, Princeton, 1950), Chap. V.

<sup>13</sup>P. Venkateswarlu, *Proc. Indian Acad. Sci. B* **25**, 119 (1947).

<sup>14</sup>P. Venkateswarlu, *Proc. Indian Acad. Sci. B* **25**, 138 (1947).

<sup>15</sup>P. Venkateswarlu, *Can. J. Phys.* **47**, 2525 (1969).

<sup>16</sup>P. Venkateswarlu, *Can. J. Phys.* **48**, 1055 (1970).

<sup>17</sup>M. J. Seaton, *Mon. Not. R. Astron. Soc.* **118**, 504 (1958).

<sup>18</sup>J. L. Dehmer and R. P. Saxon, Argonne National Laboratory Radiological & Environmental Research Division Annual Report No. ANL-8060, July 1972-June 1973, part I, p. 102.

<sup>19</sup>J. L. Dehmer (private communication).

<sup>20</sup>T. Betts and V. McKoy, *J. Chem. Phys.* **54**, 113 (1971).

<sup>21</sup>A. B. F. Duncan, *Rydberg States in Atoms and Molecules* (Academic, New York, 1971).

<sup>22</sup>The location of the lowest resonance in  $I_2$  is determined by subtracting the difference between the adiabatic and vertical ionization potentials of Potts and Price (Ref. 10), from the resonance center of Fig. 5.

<sup>23</sup>E. Lindholm, *Ark. Fys.* **40**, 97 (1969).

<sup>24</sup>T. E. H. Walker and H. P. Kelly, *J. Chem. Phys.* **57**, 936 (1972).